Environmental Pollution 244 (2019) 72–83

Contents lists available at ScienceDirect

Environmental Pollution

journal homepage: www.elsevier.com/locate/envpol

Multivariate receptor models and robust geostatistics to estimate source apportionment of heavy metals in soils☆

Jianshu Lv [a, b, *]

[a] College of Geography and Environment, Shandong Normal University, Ji'nan, 250014, China
[b] State Key Laboratory of Estuarine and Coastal Research, East China Normal University, Shanghai, 200062, China

ARTICLE INFO

Article history:
Received 12 June 2018
Received in revised form
18 September 2018
Accepted 29 September 2018
Available online 8 October 2018

Keywords:
Source apportionment
PMF
APCS/MLR
Heavy metals
Robust geostatistics

ABSTRACT

Absolute principal component score/multiple linear regression (APCS/MLR) and positive matrix factorization (PMF) were applied to a dataset consisting of 10 heavy metals in 300 surface soils samples. Robust geostatistics were used to delineate and compare the factors derived from these two receptor models. Both APCS/MLR and PMF afforded three similar source factors with comparable contributions, but APCS/MLR had some negative and unidentified contributions; thus, PMF, with its optimal non-negativity results, was adopted for source apportionment. Experimental variograms for each factor from two receptor models were built using classical Matheron's and three robust estimators. The best association of experimental variograms fitted to theoretical models differed between the corresponding APCS and PMF-factors. However, kriged interpolation indicated that the corresponding APCS and PMF-factor showed similar spatial variability. Based on PMF and robust geostatistics, three sources of 10 heavy metals in Guangrao were determined. As, Co, Cr, Cu, Mn, Ni, Zn, and partially Hg, Pb, Cd originated from natural source. The factor grouping these heavy metals showed consistent distribution with parent material map. 43.1% of Hg and 13.2% of Pb were related to atmosphere deposition of human inputs, with high values of their association patterns being located around urban areas. 29.6% concentration of Cd was associated with agricultural practice, and the hotspot coincided with the spatial distribution of vegetable-producing soils. Overall, natural source, atmosphere deposition of human emissions, and agricultural practices, explained 81.1%, 7.3%, and 11.6% of the total of 10 heavy metals concentrations, respectively. Receptor models coupled with robust geostatistics could successfully estimate the source apportionment of heavy metals in soils.

1. Introduction

Soil is the most important reservoir of pollutants in the terrestrial ecosystem, and provides a medium for the transportation of heavy metals to the atmosphere, hydrosphere, and biomass (Alloway, 2013; Kabata-Pendias and Pendias, 2001; Lv et al., 2014). Among various pollutants in soils, heavy metals are particularly hazardous due to their cumulative toxicity and persistence (Rodriguez et al., 2008); they may threaten human health through intake, direct ingestion and dermal contact (Kabata-Pendias and Mukherjee, 2007; Siegel, 2001). Heavy metals in soils are commonly controlled by both natural background and human inputs. Soil inherits the mineral skeleton of parent material through weathering and pedogenesis (Alloway, 2013), and parent materials determine the background contents of heavy metals in soils. Due to rapid industrialization and urbanization, human activities (e.g., fossils fuel combustion, industrial productions, vehicle exhaust emissions and the application of fertilizers and pesticides) inevitably lead to elevated soil heavy metal concentrations (Lv et al., 2015b; Vanek et al., 2018), which have exceeded the permissible limits for maintaining human health in some places (Chen et al., 2015; Rodríguez Martin et al., 2015; Zhong et al., 2011). Therefore, source apportionment is of key importance because it can provide references for soil management and remediation.

Multivariate statistical analyses, especially principal component analysis (PCA), have been widely used to identifying the source of heavy metals in soils (Facchinelli et al., 2001; Huang et al., 2015; Li et al., 2009; Lv et al., 2015a; Rodríguez Martín et al., 2013; Sajn et al., 2011). PCA, as a linear technique for dimensionality reduction, could transform many heavy metals into few principle component

☆ This paper has been recommended for acceptance by Prof. W. Wen-Xiong.
* College of Geography and Environment, Shandong Normal University, Ji'nan, 250014, China.
E-mail address: lvjianshu@126.com.

https://doi.org/10.1016/j.envpol.2018.09.147
0269-7491/

(PC) corresponding to a certain source. However, PCA cannot interpret the quantitative contributions of natural and human sources to heavy metals. Multivariate receptor models such as absolute principal component score/multiple linear regression (APCS/MLR) and positive matrix factorization (PMF) were developed to solve the chemical mass balance (CMB) and could quantify the source apportionment of heavy metals in soils. APCS/MLR and PMF do not depend on the previous source signatures from sampling and measurement; therefore, APCS/MLR and PMF are more convenient and efficient than traditional CMB. APCS/MLR evolved from PCA, and source contributions are obtained through carrying out the regressions between heavy metal contents and APCS (Thurston and Spengler, 1985). PMF uses experimental uncertainties in the data matrix and decomposes a data matrix into factor contributions and factor profiles under the non-negative constraint (Paatero and Tapper, 1994). Currently, APCS/MLR and PMF have been applied in source apportionment of various pollutants in the atmosphere, soil, and dust (Chen et al., 2016; Jiang et al., 2017; Lee et al., 1999; Liang et al., 2017; Lu et al., 2008; PriyaDarshini et al., 2016; Vaccaro et al., 2007; Xue et al., 2014; Zhang et al., 2012b).

Multivariate receptor models aim to create one or more new variables or factors, each representing a source with a cluster of interrelated variables within the data set (Luo et al., 2015; Qu et al., 2013; Rodríguez Martín et al., 2013). These statistical models are essential to understand the relationships between soil elements. However, these methods ignore the spatial correlations between sampling points, which contain important information. Geostatistics with variography and kriging could examine spatial structure and variability of factors resulting from multivariate receptor models (Goovaerts, 1997; Matheron, 1963), which could lead to an adequate understanding of multivariate receptor models from the insight of spatial correlations, and also facilitate to demarcate the natural or contamination source represented by respective factor. Soil data due to point-sources of pollution exhibited some hotspots or outliers. The classical Matheron's variogram, as an asymptotically unbiased estimator, is sensitive to the skewness of data due to the existence of outliers (Matheron, 1963; Webster and Oliver, 2007). Several robust estimators have been proposed to reduce the effects of the outliers in the calculation of experimental variograms (Cressie and Hawkins, 1980; Dowd, 1984; Genton, 1998). Based on robust experimental variograms fitted to theoretical models, kriged maps of the factors resulting from APCS/MLR and PMF could be superposed on the auxiliary environmental data (such as land use types and parent materials) using GIS techniques (Liu et al., 2013). Receptor models combined with robust geostatistics are expected to be powerful tools to estimate source apportionment of heavy metals in soils. To my knowledge, there are no studies conducted to apply robust geostatistics to present the result derived from receptor model.

In our study, both APCS/MLR and PMF were applied to the heavy metal datasets (As, Cd, Co, Cr, Cu, Hg, Mn, Ni, Pb, and Zn concentrations of 300 surface soils samples) in Guangrao County, eastern China, and robust geostatistics was used to map and compare the spatial structure and variability of factors resulting from the APCS/MLR and PMF. Based on these findings, potential sources represented by factors were demarcated, and sources contributions were quantified.

2. Methods and materials

2.1. Study area

Guangrao County (118°17′E~118°57′E, 36°56′N~37°21′N) is located in northern Shandong Province, eastern China, and covers approximately 1138 km^2 with a population of 0.5 million (Fig. 1). Guangrao has a temperate monsoon climate with an annual average temperature of 12.3 °C and average precipitation of 587 mm. The elevation ranges from 2 to 28 m above sea level, with a decreasing trend from southwest to northeast. Parent materials are composed of piedmont alluvium and proluvium in the southern part of the study area, bordered by Yellow River alluvium, lacustrine sediments, and marine sediments in the northern part (Fig. S1). Guangrao has well-developed agriculture in the form of grain and vegetable crops, with yields of 0.5 and 0.77 million tons, respectively (Gurangrao Municipal Bureau of Statistics, 2016). Industrial systems in the region include a coal-fired power plant, petroleum refining, and food processing, most of which are densely distributed within and around urban areas.

2.2. Soils sampling and chemical analysis

The study area was divided into 2 km × 2 km cells, and then the 300 sites were designed at the center of each cell. If the designed site was unavailable for sampling (such as if it contained a road or building), an alternative location was selected as close to the original as possible to find natural soils. At each sampling site, four to six subsamples of surface soils (0–20 cm) within a 100 m radius were collected and mixed thoroughly to obtain an approximate 1 kg sample, and root tissue, grass and leaves were discarded. The actual geographic coordinates of the sampling sites were acquired using a handheld global positioning system (GPS). Locations of 300 sampling sites are shown in Fig. 1. After air-drying, the collected soils samples were sieved to 2 mm, and ground to powder that could pass through a 0.149-mm mesh for physical-chemical analysis.

Soil pH, organic matter (OM), total nitrogen (TN), total phosphorus (TP), and $CaCO_3$ concentrations were measured according to the related literature (Lu, 2000; Lv et al., 2013). After digesting the samples using H_2SO_4-HNO_3-HF, the total concentrations of Cr, Co, Cu, Mn, Ni, V, Pb, and Zn were measured by a flame atomic absorption spectrophotometer (240 AA Agilent, USA), while Cd were analyzed by a graphite furnace atomic absorption spectrophotometer (AA-7000 Shimadzu, Japan). Hg concentrations were measured by an atomic fluorescence spectrometer (AFS230E Haiguang Analytical Instrument Co., Beijing, China) following the digestion of H_2SO_4-HNO_3-$KMnO_4$ (Lu, 2000). Analytical reagent blanks were applied in the sample preparation and analytical processes. All measurements were performed in triplicate, and standard deviations were within ±5% of the mean. The standard reference material (GSS-1) was used to control the measurement errors, with recoveries of 100% ± 10% for 10 heavy metals.

2.3. Receptor models

2.3.1. APCS/MLR

APCS/MLR, derived from the traditional PCA (Paatero and Tapper, 1994), was performed using SPSS 16.0 software (SPSS Inc., USA). First, the raw data are normalized as following:

$$Z_{ij} = \frac{C_{ij} - \overline{C}_j}{\delta_j} \quad (1)$$

where C_{ij} is the concentration of the jth metal in ith sample, $\overline{C}_j$ is the mean concentration of the jth metal for all samples, and δ_j is the standard deviation of jth metal.

An artificial sample with all concentrations of 0 is introduced and is also normalized:

$$Z_0 = \frac{0 - \overline{C}_j}{\delta_j} = \frac{-\overline{C}_j}{\delta_j} \quad (2)$$

The APCS for the factors are estimated by subtracting the factor scores of Z_0 from the factor scores of true samples. The contributions to C_j can be obtained by using a multiple linear regression according to the equation below:

$$C_j = b_0 + \sum_{k=1}^{p} b_k APCS_k \quad (3)$$

where b_0 is the intercept of regression for jth element, b_k is the regression coefficient, p is the number of factors, $b_k APCS_k$ is the contribution of the pth factor to Cj, and the average value of $b_k APCS_k$ represents the mean contribution of the pth factor to Cj.

2.3.2. PMF

PMF modeling was performed using the US-EPA PMF 5.0 program (U.S. Environmental Protection Agency, 2014). PMF is a multivariate factor analysis tool to solve the CMB, and the initial data matrix X with the order of $m \times n$ can be expressed as:

$$X = GF + E \quad (4)$$

$G\,(m \times p)$ is the matrix of the factor contribution, $F\,(p \times n)$ is the matrix of the factor profile, and $E\ (m \times n)$ is the residual error matrix.

E can be written as:

$$e_{ij} = \sum_{k=1}^{p} g_{ik} f_{kj} - x_{ij} \quad (5)$$

where i represents elements 1 to m, j represents elements 1 to n, and k represents the source from 1 to p.

Factor contributions and profiles are acquired by the PMF model minimizing the objective function Q under the constraint of non-negative contributions, and the solution in the US-EPA PMF program is approximated by Multilinear Engine-2 (ME-2) (Paatero, 1999).

$$Q = \sum_{i=1}^{n} \sum_{j=1}^{m} \left(\frac{e_{ij}}{u_{ij}} \right)^2 \quad (6)$$

where u_{ij} is the uncertainty in the jth chemical element for sample i.

The uncertainty is calculated based on the element-specific method detection limit (MDL), and error percent is measured by standard reference materials. Because all the measured contents are above the MDL, the equations of uncertainty are adopted as following:

$$Unc = \sqrt{(ErrorFraction \times concentration)^2 + (0.5 \times MDL)^2} \quad (7)$$

The US-EPA PMF 5.0 program contains a rotation tool that sets an Fpeak value in order to improve oblique edges (Paatero and Hopke, 2009; Paatero et al., 2002; U.S. Environmental Protection Agency, 2014). Positive Fpeak values sharpen the F and smear the G, while negative Fpeak values have a contrasting transformation.

2.4. Robust geostatistical method

The APCS, PMF-factors and 10 heavy metals were analyzed for their spatial structure and variability. Four experimental variograms including Matheron's estimator (Matheron, 1963) and three robust estimators (Cressie and Hawkins's estimator (Cressie and Hawkins, 1980), Dowd's estimator (Dowd, 1984), and Genton's estimator (Genton, 1998)) were used to build the degree of spatial continuity and to analyze the range of spatial dependence for APCS and PMF-factors, which were fitted to Spherical, Gaussian and Exponential and Matérn models, respectively. Cressie and Hawkins' estimator essentially damps the effect of outliers from the

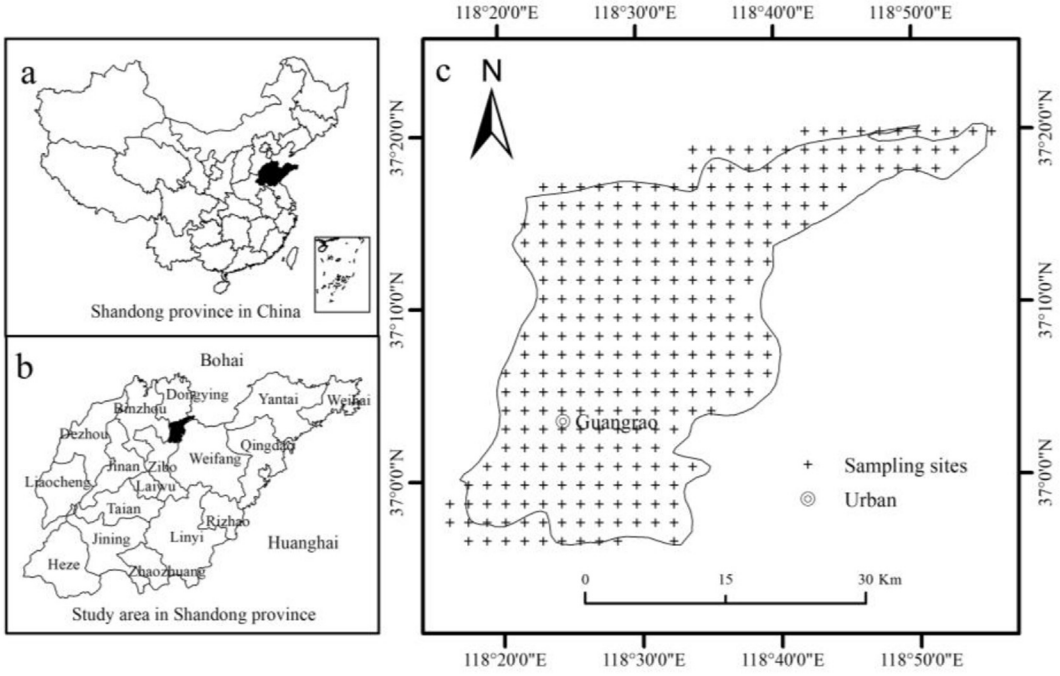

Fig. 1. The location of study area with sampling sites. a) The location of Shandong province in China, b) the location of Guangrao in Shandong province, c) the location of 300 sampling sites in Guangrao.

secondary process, and is based on the fourth root of the squared differences. Dowd's estimator and Genton's estimator are both scale estimators, they estimate the variogram for a dominant intrinsic process in the presence of outliers. For detailed descriptions of these four estimators, please refer to the related literature (Cressie and Hawkins, 1980; Dowd, 1984; Genton, 1998; Goovaerts, 1997; Webster and Oliver, 2007). Experimental variograms were calculated using the Georob package (Papritz and Schwierz, 2018) in R 3.3.2 software (R Development Core Team).

The median of the squared deviation ratio (SDR) derived from cross-validation was used to find the best association of the experimental variogram fitted to the theoretical model. When the best association is used for kriging, the median of SDR should be close to 0.455 (Lark, 2000).

$$SDR = \frac{\left(z(x_\alpha) - z^*(x_\alpha)\right)^2}{\sigma^2 KR(x_\alpha)} \quad (8)$$

Kriged estimation is expressed as the weighted sums of the adjacent sampled concentrations with different kriging algorithms (Goovaerts, 1997), and ordinary kriging (OK) was conducted using ArcGIS 10.2 (Esri Inc., USA).

3. Results

3.1. Descriptive statistics of soil properties and heavy metals

Descriptive statistics of physical-chemical properties and heavy metals in Guangrao are summarized in Table 1. The mean pH of 8.24 suggested that the surface soils had completely alkaline properties, which commonly reduces the mobility of heavy metals (Alloway, 2013). OM with a mean value of 1.45% was higher than the background values of Shandong Province (China National Environmental Monitoring Center, 1990). The mean contents of TN and TP in topsoil samples were 0.90 and 0.97 g kg^{-1}, which were higher than their background values (China National Environmental Monitoring Center, 1990). The mean content of $CaCO_3$ was 8.66%, varying between 2.48% and 18.95%, and thus the soils showed relatively high $CaCO_3$ levels.

The mean concentrations of As, Cd, Co, Cr, Cu, Hg, Mn, Ni, Pb and Zn were 10.8, 0.13, 11.9, 68.1, 24.0, 0.04, 586, 28.8, 22.6 and 67.2 mg kg^{-1}, respectively. The contents of As, Cd, Cr, Cu, Ni, Pb and Zn in all samples were below level II of the Environmental Quality Standard for Soils (EQSS) of China (State Environmental Protection Administration of China, 1997), which represents the threshold to maintain safety in agricultural production and human health, and there was only one sample with a Hg content slightly above level II of the EQSS. The average contents of As, Cd, Cr, Cu, Hg, Mn, Ni, and Zn exceeded the corresponding background values of Shandong Province (China National Environmental Monitoring Center, 1990): in particular, the mean contents of Cd and Hg presented at 1.86 and 2.5 times the background values, suggesting that these two heavy metals were clearly enriched in topsoils. Hg had the highest coefficient of variation (CV), followed by Cd, reflecting a wider extent of variability in relation to the means. Hg and Cd showed strongly positive skewness, which may be attributed to the outliers from human inputs (Lv et al., 2013).

Analysis of variance (ANOVA) was applied to examine the differences of soil heavy metal concentrations between parent materials and among land use types (Table S1). No significant differences were observed for As, Co, Cu, and Pb among land use types. Significantly, while urban areas presented the lowest Cr, Mn, Ni and Zn contents and the highest Hg concentration, cultivated land exhibited the highest Cd content. As, Cd, Co, Cr, Cu, Mn, Ni, Pb and Zn presented significantly higher contents in the soils from lacustrine deposit and the Yellow River alluvium. For Hg, there were no significant differences among parent materials.

3.2. APCS/MLR modeling

The first three factors were extracted through PCA (Table S2) and explained 83.5% of the total variance. Approximately, 64.8% of total variance was explained by Factor 1 (F1), showing strongly positive loadings of As, Co, Cr, Cu, Mn, Ni, Pb, and Zn, as well as moderate loading of Cd. F2, accounting for 11.5% of the total data variance, had highly positive loadings of Hg and a moderate loading of Pb. F3 amounted to 7.2% of the total variance and was dominated exclusively by the moderate loading of Cd.

The results of APCS/MLR modeling are shown in Table 2, and Table S3. R^2 and the ratio of predicted to observed values were used to assess the accuracy of APCS/MLR modeling. These two parameters varied between 0.63 and 0.94, 0.87 and 1.08, respectively, indicating that APCS-MLR modeling had high accuracy (Table 2). The results of APCS/MLR were consistent with PCA. There were some negative values explained by F2 and F3, resulting in the As, Co, Cu, Mn, Ni, and Zn contents explained by F1 exceeding their total predicted values. All heavy metals except for Hg were primarily contributed by F1, and ranged from 50.4% to 130.1%. Hg exhibited the highest concentration in F2, and was thus dominated by F2. F2 explained 15.9% of Pb concentration (3.6 mg kg^{-1}). F3

Table 1
Descriptive statistics of physical-chemical properties and heavy metals in soils.

	Unit	Range	Mean	Median	SD	Skewness	Kurtosis	CV	Background [a]	Level II of EQSS [b]
pH	–	7.81–8.75	8.24	8.22	0.18	0.28	−0.17	0.02	–	–
OM	%	0.14–3.41	1.43	1.45	0.43	−0.02	2.02	0.30	1.31	–
TN	g kg^{-1}	0.20–1.66	0.90	0.93	0.23	−0.70	1.128	0.25	0.82	–
TP	g kg^{-1}	0.48–2.32	0.97	0.94	0.26	1.16	2.64	0.27	0.66	–
$CaCO_3$	%	2.48–18.95	8.66	9.00	2.75	0.07	−0.42	0.32	–	–
As	mg kg^{-1}	5.2–17.2	10.8	10.3	2.64	0.44	−0.5	0.24	8.9	30
Cd	mg kg^{-1}	0.07–0.29	0.13	0.13	0.03	1.1	2.54	0.25	0.07	0.3
Co	mg kg^{-1}	6.1–16.9	11.9	11.9	1.83	−0.15	0.22	0.15	12.6	–
Cr	mg kg^{-1}	53.5–94.1	68.1	67.5	5.53	0.54	1.08	0.08	64.3	200
Cu	mg kg^{-1}	11.8–37.8	24.0	23.7	4.42	0.14	0.69	0.18	22.3	100
Hg	mg kg^{-1}	0.01–0.54	0.04	0.03	0.04	9.99	128.71	0.95	0.016	0.5
Mn	mg kg^{-1}	411–970	586	576	98.46	0.91	1.11	0.17	552.00	–
Ni	mg kg^{-1}	14.6–43.4	28.8	28.6	5.05	0.09	0.01	0.18	24.4	50
Pb	mg kg^{-1}	12.6–30.4	22.6	22.8	2.99	−0.77	1.36	0.13	24.5	300
Zn	mg kg^{-1}	34.8–98.6	67.2	66.6	10.63	−0.08	0.29	0.16	60.9	250

[a] Soil background values of Shandong province (China National Environmental Monitoring Center, 1990).
[b] Level II of the Environmental Quality Standard for Soils (EQSS) of China (State Environmental Protection Administration of China, 1997).

Table 2
Percentage contribution (%) of each factor for heavy metals derived from APCS/MLR and PMF.

	APCS/MLR						PMF				
	Predicted/Observed	R^2	F1	F2	F3	Unidentified	Predicted/Observed	R^2	F1	F2	F3
As	1.00	0.74	115.4	−2.0	4.7	−18.0	1.00	0.98	84.2	7.0	8.8
Cd	1.08	0.88	75.2	1.5	35.9	−12.6	1.03	0.99	61.3	9.1	29.6
Co	0.87	0.89	116.3	0.0	−27.3	11.0	0.99	0.90	81.8	7.7	10.4
Cr	1.00	0.63	50.4	−0.9	4.9	45.7	0.99	0.62	77.3	8.9	13.8
Cu	0.98	0.89	130.1	−1.2	−3.8	−25.1	0.98	0.88	78.9	9.6	11.4
Hg	0.93	0.88	12.5	47.9	9.3	30.3	0.94	0.57	47.0	43.1	9.9
Mn	1.00	0.86	114.0	−1.4	0.7	−13.4	1.00	0.89	81.9	6.6	11.5
Ni	1.11	0.93	110.8	−0.7	5.1	−15.2	0.99	0.93	82.3	7.0	10.7
Pb	1.00	0.71	73.5	15.9	−2.5	13.1	0.99	0.80	75.1	13.2	11.7
Zn	1.00	0.94	111.8	0.6	−5.2	−7.2	0.99	0.93	80.0	8.8	11.2
∑metals	–	–	107.5	−1.1	0.5	−6.9	–	–	81.1	7.3	11.6

contributed to the 35.9% of Cd variation but explained very small proportions of the other nine heavy metals. The unaccounted part, referring to the intercepts of regressions, varied from −25.1% to 45.7%, with the highest values for Cr. The source contributions to Σ metals of the three factors were also calculated by the APCS/MLR. F1 dominated the Σ metals with the contribution of 107.5%, while F2 and F3 explained merely −1.1% and 0.5% of the Σ metals.

3.3. PMF modeling

PMF modeling with the use of three factors was determined by trying factor numbers ranging from 1 to 6, and then using the rotational tool when running the model to improve oblique edges (Paatero and Hopke, 2009). The optimal three factors were derived from a run with the Fpeak of −0.5 and Q (robust) of 3257 and are shown in Table 2, and Table S3. The ratios of predicted to observed values were close to 1, and R^2 varied between 0.57 and 0.99; indicating a good fit for PMF modeling (Table 2). As, Cd, Co, Cr, Cu, Mn, Ni, Pb, and Zn had the highest concentrations in F1 and were influenced by F1 with a contribution ranging from 61.3% to 84.2%. F1 contributed to 47.0% of the Hg variation, roughly equivalent to F2 (43.1%), and Pb had 13.2% of concentration related to F2. F3 dominated 29.6% of Cd and presented small contributions to other heavy metals. The strongest contribution to the ∑ metals in soils was F1, with a contribution of 81.1%, followed by F3 (11.6%) and F2 (7.3%) in turn.

The results calculated from PMF were consistent with APCS/MLR in terms of three factors. However, APCS/MLR had some negative contributions and unidentified parts and may have some limits. F1 arising from two models commonly showed high contributions for As, Cd, Co, Cr, Cu, Mn, Ni, Pb, and Zn. Hg and Pb were significantly explained by both F1 and F2, while F3 had the highest relation for Cd only.

3.4. Geostatistical analysis

The results of variogram fitting for APCS and PMF-factors are indicated in Fig. 2 and Table S4. Through comparing the median of SDR with 0.455, Dowd's variogram fitted to a Gaussian model were the best for APC1 and APC3, and Genton's variogram fitted to an exponential model was the most suitable for APC2. Dowd's variogram fitted to spherical and Gaussian models were used for PMF-F1 and PMF-F2, while Genton's variogram fitted to a Gaussian model corresponded to PMF-F3. The experimental variograms of corresponding APCS and PMF-factors showed their significant differences (Fig. 2), which could be attributed to the different algorithms of PMF and ACPS/MLR. The nugget/sill ratio can be regarded a parameter to classify the spatial dependence of soil factors. The nugget/sill ratio varied from 0.365 for APC 1 and 0.622 for PMF-F1, 0.196 for APC 2 and 0.455 for PMF-F2, 0.536 for APC 3 and 0.265 for PMF-F3, indicated the different spatial dependence of corresponding APCS and PMF-factor. Range is another important geostatistical parameter considered to be the distance beyond which observations are not spatially dependent. The ranges of APC 1 and PMF-F1, APC 3 and PMF-F3 were similar, but APC 2 and PMF-F2 were different. The variogram fitting results for log-transformed heavy metals are shown in Table S5 and Fig. 3. The best associations of experimental variograms fitted to theoretical models differed among 10 heavy metals.

Kriged maps of APCS, PMF-factors and 10 heavy metals are illustrated in Fig. 4 and Fig. 5. It is clearly implied that the spatial distribution of APCS was quietly in accordance with the corresponding PMF-factor (Fig. 4). Furthermore, heavy metals and their corresponding APCS and PMF-factor had analogous distributions (Figs. 4 and 5). APC 1, PMF-F1, As, Cd, Co, Cr, Cu, Mn, Ni, Pb, and Zn showed similar patterns (Fig. 4a1, b1 and 5a, b, c, d, e, g, h, i, j) and were characterized by the significant north-south trend with higher values in the north part, which coincided with parent materials (Fig. S1b). The common hotspot of APC2, PMF-F2, Hg and Pb was located at the southwest region corresponding to nearby urban areas and followed a decreasing trend from the center to the periphery (Fig. 4a2, b2, and 5f, i). APC3, PMF-F3 and Cd presented high values in the northern and southern zones, as well as low values in the central region (Fig. 4a3, b3, and 5b).

4. Discussion

4.1. Source interpretation of factor 1

As, Cd, Cu, Mn, Pb, and Zn associated with Co, Cr and Ni had high and positive loadings in the F1 (Table 2, and Table S3) through PMF and APCS/MLR modeling, and the contributions of F1 to these heavy metals by PMF were close to the respective background values (Table 1), suggesting a strong lithogenic source of this group of nine heavy metals by the parent materials (Nanos and Rodríguez Martin, 2012). The concentrations of Co, Cr and Ni in soils highly rely on their contents in parent rocks, and human inputs of Co, Cr and Ni from fertilizers, limestone, and manure are commonly lower than their background contents in soils (Alloway, 2013; Facchinelli et al., 2001; Rodríguez Martín et al., 2006). Co, Cr and Ni grouped in the same factor by the PCA and PMF are commonly considered as the indicator of a natural source, which has been clearly demonstrated by the works of Rodríguez Martín et al. (2006) in the Ebro river basin, Nanos and Rodríguez Martin (2012) in the Duero river basin, Lv et al. (2015a) in Ju County, Facchinelli et al. (2001) in Piemonte, Xue et al. (2014) in Changxing, and Jiang et al. (2017) in Changshu.

Based on kriged maps of APCS and PMF-factors and ANOVA results (Fig. 4, Table S1), we confirmed that As, Cd, Co, Cr, Cu, Mn, Ni,

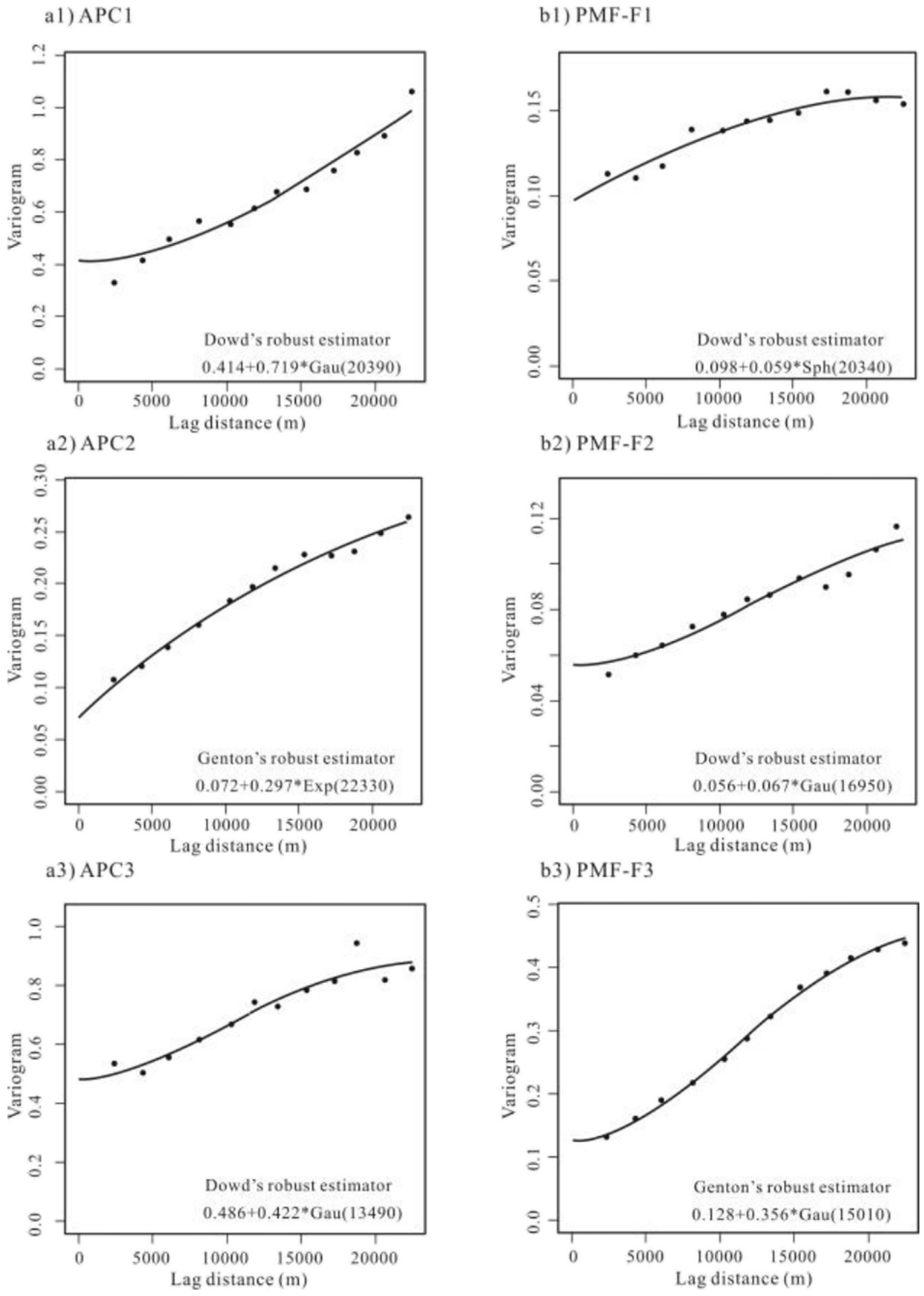

Fig. 2. The best association of experimental variograms fitted to theoretical models for APCS and PMF-factors. a1) APC1, a2) APC2, a3) APC3, b1) PMF-F1, b2) PMF-F2. The solid point represents the experimental variogram. The solid line indicates fitted theoretical model.

Pb, and Zn were grouped in a lithologic factor. Through spatial overlay analysis on kriged maps and parent materials (Fig. 4a1, 4b1, Fig S1b), it was found that kriged maps of APC1 and PMF-F1 coincided with spatial patterns of parent materials, with higher values in the northern soils originating from lacustrine sediments and Yellow River alluvium rather than piedmont alluvium and proluvium and marine sediments, which is consistent with the ANOVA. The study area is covered by four types of quaternary sediments with a similar material origin from the northern mountains (Fig. S1b), but their grain sizes differ due to sedimentary dynamics, leading to the differences in heavy metal contents in soils. Lacustrine sediments and Yellow River alluvium tend to contain more fine-grained fractions than marine sediments and alluvial-proluvial deposits (China National Environmental Monitoring Center, 1990).

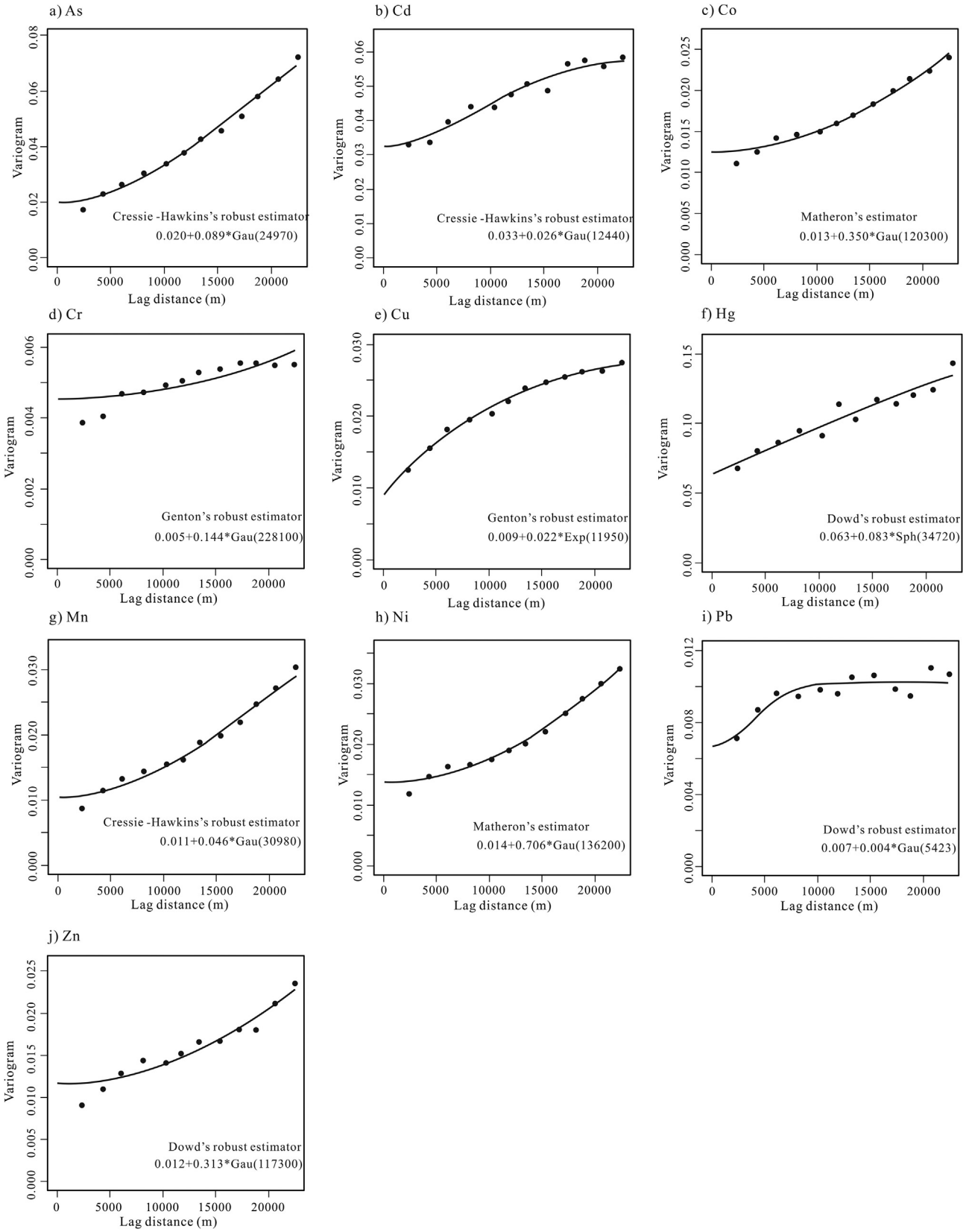

Fig. 3. The best association of experimental variograms fitted to theoretical models for log-transformed concentrations of As (a), Cd (b), Co (c), Cr (d), Cu (e), Hg (f), Mn (g), Ni (h), Pb (i), and Zn (j). The solid point represents the experimental variogram. The solid line indicates fitted theoretical model.

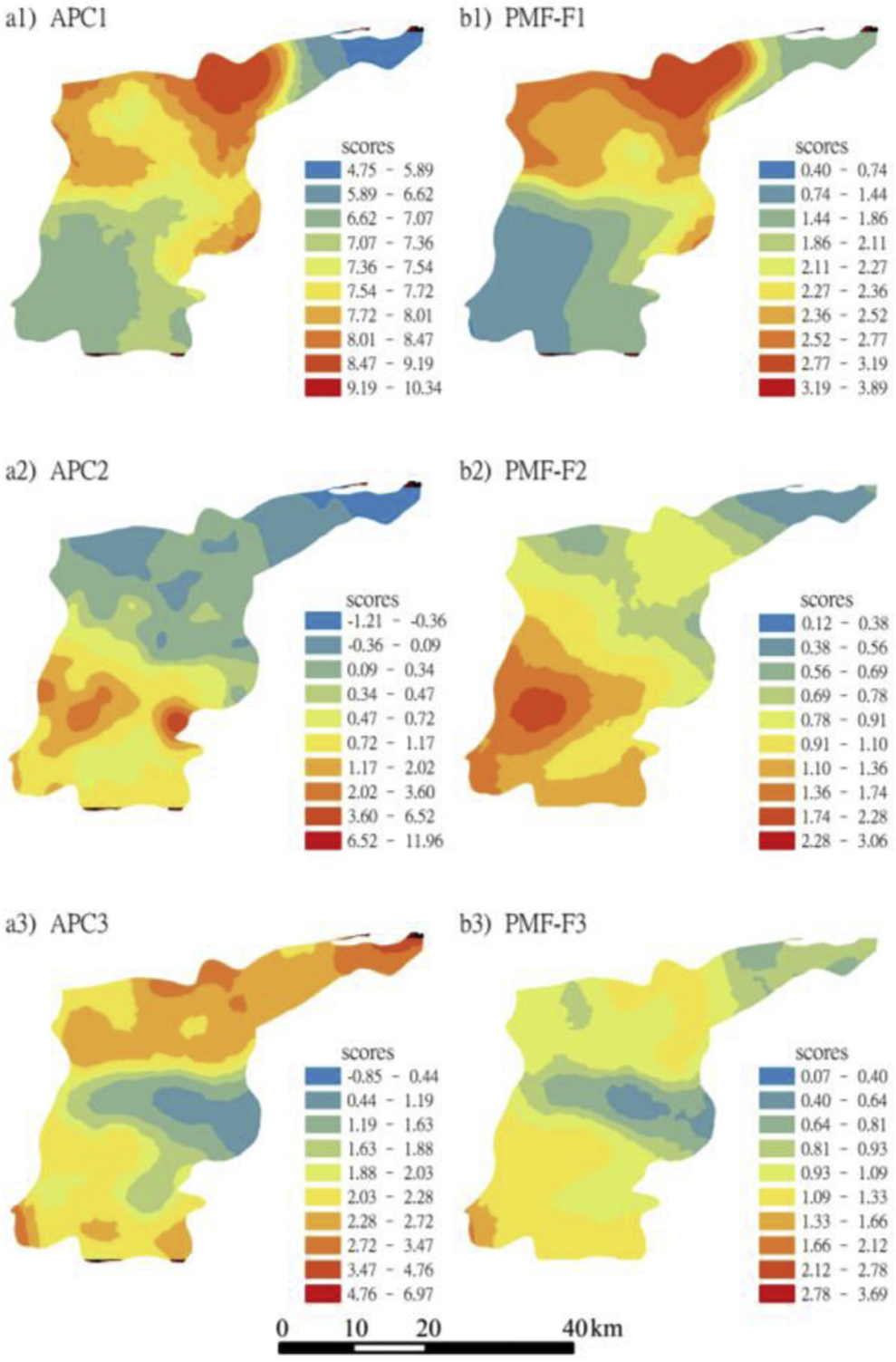

Fig. 4. Kriged interpolation of APCS and PMF-factors. a1) APC1, a2) APC2, a3) APC3, b1) PMF-F1, b2) PMF-F2, and b3) PMF-F3.

It is well known that heavy metals have higher concentrations in fine-grained sediments and lower levels in coarse-grained sediments because fine-grained sediments with a higher clay fraction have a stronger ability to adsorb heavy metals in sedimentary processes (Alloway, 2013). Lv and Yu (2018) also found that the soils from lacustrine sediments exhibited higher heavy metals contents than those of marine sediments and alluvial-proluvial deposits. Therefore, it seemed reasonable to conclude that F1 represented the natural source.

4.2. Source interpretation of factor 2

F2 was highly related to Hg in APCS/MLR and PMF, indicating that F2 may represent an anthropic source (Table 2, and Table S3).

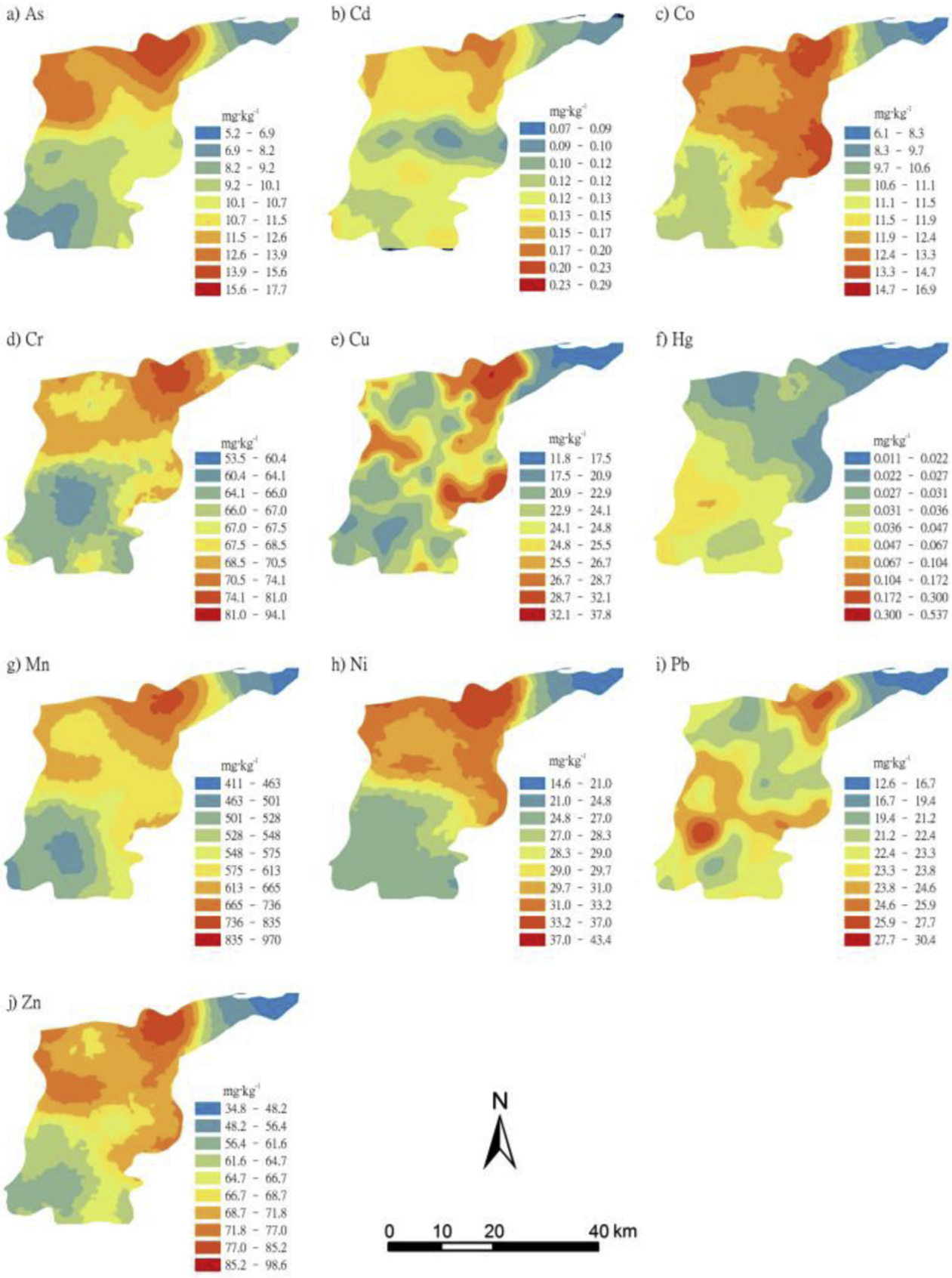

Fig. 5. Kriged interpolation of the concentration of As (a), Cd (b), Co (c), Cr (d), Cu (e), Hg (f), Mn (g), Ni (h), Pb (i), and Zn (j).

The mean concentration of Hg was almost two times the background value of Shandong Province with the maximum value of 0.537 mg kg^{-1}, and 43.1% of the Hg concentration was explained by PMF-F2. The hotspots for APC2, PMF-F2 and Hg were exclusively located around urban areas with dense industrial factories and traffic lines (Fig. 4a2, 4b2, 5f, and Fig S1a), and Hg was 0.09 mg kg^{-1} in urban areas, which is almost 6 times more than the background values (Table 1, Table S1). The anthropic sources of Hg in PCA have been clearly demonstrated in previous works (Cai et al., 2012; Lv et al., 2013), where Hg was grouped in an isolated factor. It could be inferred that F2 may represent the atmospheric deposition of human emissions.

There are several coal-fired plants and factories in Gurangrao with an annual consumption of 2 million tons (Gurangrao Municipal Bureau of Statistics, 2016), and coal combustion is commonly regarded as the most important source of Hg in China (Wu et al., 2016; Ying et al., 2017; Zheng et al., 2011). The average Hg concentration in coal in China is 0.17 mg kg^{-1} (Zhang et al., 2012a). The chemical behaviors of Hg in the combustion process are significantly different from other metals due to its high volatility (Vejahati et al., 2010; Xu et al., 2004). At temperatures over 700 °C, almost 100% of Hg in coal is output to flue gas with three types of speciation, including gaseous elementary Hg (Hg^0), gaseous oxidized Hg (Hg^{2+}), and particle-bound Hg (Wang et al., 2012; Xu et al., 2004; Zhu et al., 2016). Particle-bound Hg and gaseous Hg^{2+} could be effectively captured by the electrostatic precipitators (ESP) and wet flue gas desulfurization (WFGD), respectively, which have been equipped in the coal-fired power plants and factories in Guangrao. However, the water-insoluble Hg^0 is resistant to being captured by the ESP and WFGD, and can easily escape to the atmosphere. Srivastava et al. (2006) reported that ESP and ESP +WFGD could remove only 38.6% and 46.9% of Hg in flue gas, respectively. Hg^0 accounts for more than 70% of the total Hg emission from coal combustion after the retaining of scrubbers (Yang et al., 2012). Hg in the atmosphere could enter soils through dry and wet atmospheric deposition (Lindberg et al., 2007; Lv et al., 2013), and Rodríguez Martin and Nanos (2016) found that most of the emitted mercury was deposited within 15 km from the power plants. As, Cd, Co, Cr, Cu, Mn, Ni, Pb, and Zn are mid- or low-volatile elements (Xu et al., 2004) and are mainly distributed in the fly ash and bottom ash with little vapor in the coal-fired process; ESP+WFGD scrubbers are sufficient to remove these metals in flue gas (Zhu et al., 2016). Deng et al. (2014) found that the percentages of removal for Pb, Mn and Cd through ESP+WFGD reached 95–99% in six coal-fired power plants in China. Zhao et al. (2017) found that the overall removal rates of Cr, Mn, Co, Ni, Cu, Zn, As, Ba, and Pb by ESP+WFGD were higher than 99.9% in a 100 MW coal-fired power plant. Therefore, coal combustion contributed a much higher proportion of Hg compared with the other nine metals.

Additionally, there are 10 oil-refining factories in the region due to its proximity to the Shengli oil field, the second largest oil field in China, with a total annual crude oil-processing capacity of approximately 3 million tons (Gurangrao Municipal Bureau of Statistics, 2016). Heavy metals with medium and low volatilities combined with sulfur and nitrogen could be effectively removed by hydro-processing (HDT), with the exception of the highly volatile Hg (Zheng et al., 2011). According to the work of Wilhelm in the USA (Wilhelm, 2001), approximately 20% of Hg in crude oil escapes to the atmosphere in the refining process, approximately 25% is contained in solid and liquid waste from refineries, and approximately 55% is finally deposited in products on the market. Therefore, oil-refining processes could be another source of Hg.

After analyzing coal combustion and oil refining processes, it is clear that both of these two human inputs contributed a much higher proportion of Hg than other heavy metals due to its high volatility, which is consistent with the findings of exclusively high Hg loading in F2 and relatively low loading of other heavy metals in PMF and APCS/MLR. Additionally, 13.2% of Pb concentration was controlled by F2 in PMF modeling, and Pb had a hotspot with high values in the urban area (Fig. 5i), suggesting that F2 was also related to traffic emissions. Tetraethyl lead was historically used as an antiknock agent in gasoline, where it was emitted into the atmosphere through combustion and then entered soils through atmospheric deposition. Though tetraethyl lead has been banned in China since 2000 (Chen et al., 2012), the historical Pb emissions from vehicles still exist in soils. Consequently, we confirmed that F2 was related to the dry and wet atmospheric deposition of coal combustions, oil refining and traffic emissions.

4.3. Source interpretation of factor 3

F3 was dominated exclusively by Cd in PCA and PMF and explained 29.6% of the Cd concentration in PMF modeling (Table 2, and Table S3). The high values of APC3, PMF-F3 and Cd were distributed in the central and north parts of the study area (Fig. 4a3, 4b3, 5b, and Fig. S1b), coinciding with the spatial distribution of vegetable-producing soils. The amount of fertilizer applications in vegetable-producing soils is 5–10 times greater than that of other cultivated land to maintain this area's vast productivity (Liu et al., 2008). Cd, as an inherent component of phosphate rock, is transferred to phosphate fertilizers (Mortvedt, 1996; Nziguheba and Smolders, 2008), and thus Cd is commonly an indicator of the application of chemical fertilizers. The application of chemical fertilizers on the study area in 2016 was 1468 kg hm^{-2}, and the phosphate, nitrate, potassium, and compound fertilizers accounted for 33.6%, 19.9%, 8.7% and 37.8% of the total application amount, respectively (Gurangrao Municipal Bureau of Statistics, 2016). In China, the mean Cd contents in phosphate rock and phosphate fertilizer are 0.98 and 0.6 mg kg^{-1} (Lu et al., 1992), and compound fertilizers have a mean Cd content of 0.18 mg kg^{-1} (Wang and Ma, 2004), which is much higher than the background values in soils (Table 1). Meanwhile, the mean Cd contents in the nitrate and potassium fertilizers are 0.0005 and 0.05 mg kg^{-1}, significantly lower than those in phosphate and compound fertilizers and the background values in soils. The levels of Cu, Hg, Mn, Pb and Zn in all four fertilizers are lower than their background values in soils. Therefore, the application of chemical fertilizers could elevate Cd levels in agricultural soils more significantly than other metals, in agreement with the prominent loading of Cd in F3. Rodríguez Martín et al. (2013), Gil et al. (2004), Lu et al. (2012), Chen et al. (2008), and Lv et al. (2015a) found that Cd combined with other metals in the same group could indicate inputs from agricultural practices. It could be concluded that F3 represented agricultural practices.

4.4. Source contribution of heavy metals in soils

Once we determined the sources related to various factors, the source contributions of heavy metals could be easily determined. PMF and APCS/MLR afforded three similar factors with comparable contributions. PMF were calculated under the circumstances of a non-negative constraint; therefore, the contributions values from PMF were all non-negative, while APCS/MLR showed some negative and unidentified contributions. Therefore, PMF could provide more rational source contributions than APCS/MLR and was adopted for source apportionment. Khairy and Lohmann (2013), Sofowote et al. (2010), Sofowote et al. (2008), Stout and Graan (2010) found that PMF could afford better source apportionment of pollutants in the atmosphere, soils and sediments than APCS/MLR.

Co, Cr, Cu, Mn, Ni, and Zn were dominated by parent materials, with their contributions varying from 77.3% to 84.2%, and mainly originated from a natural source. Hg originated equally from the parent materials and atmospheric deposition of human emissions, with contributions of 47.0% and 43.1%, respectively. Pb was explained by parent materials with a contribution of 75.1%, but atmospheric deposition from human emissions also accounted for 13.2% of Pb. Cd was mainly controlled by parent materials and agricultural practices, with percentages of 61.3% and 29.6%, respectively. In total, 81.1% of the sum of heavy metal contents originated from natural sources, and atmospheric deposition of human emissions and agricultural practices contributed only 7.3% and 11.6% of the total heavy metal contents.

5. Conclusions

In this study, we combined two multivariate receptor models and robust geostatistics to estimate source apportionment of heavy metals in soils of Guangrao, eastern China. PMF with the non-negative constraint afforded better source apportionment results than APCS/MLR. Although the best association of experimental variograms fitted to theoretical models differed between the corresponding APCS and PMF-factors, they showed similar spatial variability. Three sources were determined including natural source, atmosphere deposition of human emissions, and agricultural practices, explaining 81.1%, 7.3%, and 11.6% of the total of 10 heavy metals concentrations, respectively. Parent material was the dominate source of As, Co, Cr, Cu, Mn, Ni, and Zn, with the contributions varying from 77.3% to 84.2%. Hg originated from equally parent materials (47.0%) and atmosphere deposition of human emissions (43.1%). 75.1% of Pb concentration was associated with parent materials, and was also influenced by atmosphere deposition of human inputs (13.2%). Cd was related to parent materials and agricultural practices, with the contribution of 61.3% and 29.6%, respectively.

Acknowledgement

This study was jointly funded by National Natural Science Foundation of China (No. 41601549), Natural Science Foundation of Shandong Province (No.ZR2016DQ11), and Open Research Fund of State Key Laboratory of Estuarine and Coastal Research (SKLEC-KF201710).

Appendix A. Supplementary data

Supplementary data to this article can be found online at https://doi.org/10.1016/j.envpol.2018.09.147.

References

Alloway, B., 2013. Heavy Metals in Soils. Springer, Dordrecht.
Cai, L.M., Xu, Z.C., Ren, M.Z., Guo, Q.W., Hu, X.B., Hu, G.C., Wan, H.F., Peng, P.G., 2012. Source identification of eight hazardous heavy metals in agricultural soils of Huizhou, Guangdong Province, China. Ecotoxicol. Environ. Saf. 78, 2–8.
Chen, H.Y., Teng, Y.G., Chen, R.H., Li, J., Wang, J.S., 2016. Contamination characteristics and source apportionment of trace metals in soils around Miyun Reservoir. Environ. Sci. Pollut. Res. 23, 15331–15342.
Chen, H.Y., Teng, Y.G., Lu, S.J., Wang, Y.Y., Wang, J.S., 2015. Contamination features and health risk of soil heavy metals in China. Sci. Total Environ. 512, 143–153.
Chen, T., Liu, X.M., Zhu, M.Z., Zhao, K.L., Wu, J.J., Xu, J.M., Huang, P.M., 2008. Identification of trace element sources and associated risk assessment in vegetable soils of the urban-rural transitional area of Hangzhou, China. Environ. Pollut. 151, 67–78.
Chen, X.D., Lu, X.W., Yang, G., 2012. Sources identification of heavy metals in urban topsoil from inside the Xi'an Second Ringroad, NW China using multivariate statistical methods. Catena 98, 73–78.
China National Environmental Monitoring Center, 1990. Background Concentrations of Elements in Soils of China. China Environmental Science Press, Beijing.
Cressie, N., Hawkins, D.M., 1980. Robust estimation of the variogram.1. Math. Geol. 12, 115–125.
Deng, S., Shi, Y.J., Liu, Y., Zhang, C., Wang, X.F., Cao, Q., Li, S.G., Zhang, F., 2014. Emission characteristics of Cd, Pb and Mn from coal combustion: field study at coal-fired power plants in China. Fuel Process. Technol. 126, 469–475.
Dowd, P.A., 1984. The variogram and kriging: robust and resistant estimators. In: Verly, G., David, M., Journel, A.G., Marechal, A. (Eds.), Geostatistics for Natural Resources Characterization (Part 1). Reidel, Dordrecht, pp. 91–106.
Facchinelli, A., Sacchi, E., Mallen, L., 2001. Multivariate statistical and GIS-based approach to identify heavy metal sources in soils. Environ. Pollut. 114, 313–324.
Genton, M.G., 1998. Highly robust variogram estimation. Math. Geol. 30, 213–221.
Gil, C., Boluda, R., Ramos, J., 2004. Determination and evaluation of cadmium, lead and nickel in greenhouse soils of Almeria (Spain). Chemosphere 55, 1027–1034.
Goovaerts, P., 1997. Geostatistics for Natural Resources Evaluation. Oxford University Press, New York.
Gurangrao Municipal Bureau of Statistics, 2016. Gruangrao Statistical Year Book in 2016. China Statistics Press, Beijing.
Huang, Y., Li, T.Q., Wu, C.X., He, Z.L., Japenga, J., Deng, M., Yang, X., 2015. An integrated approach to assess heavy metal source apportionment in pen-urban agricultural soils. J. Hazard Mater. 299, 540–549.
Jiang, Y.X., Chao, S.H., Liu, J.W., Yang, Y., Chen, Y.J., Zhang, A.C., Cao, H.B., 2017. Source apportionment and health risk assessment of heavy metals in soil for a township in Jiangsu Province, China. Chemosphere 168, 1658–1668.
Kabata-Pendias, A., Mukherjee, A.B., 2007. Trace Elements from Soil to Human. Springer Verlag, Berlin.
Kabata-Pendias, A., Pendias, H., 2001. Trace Elements in Soils and Plants. CSC press, London.
Khairy, M.A., Lohmann, R., 2013. Source apportionment and risk assessment of polycyclic aromatic hydrocarbons in the atmospheric environment of Alexandria, Egypt. Chemosphere 91, 895–903.
Lark, R.M., 2000. A comparison of some robust estimators of the variogram for use in soil survey. Eur. J. Soil Sci. 51, 137–157.
Lee, E., Chan, C.K., Paatero, P., 1999. Application of positive matrix factorization in source apportionment of particulate pollutants in Hong Kong. Atmos. Environ. 33, 3201–3212.
Li, J.L., He, M., Han, W., Gu, Y.F., 2009. Analysis and assessment on heavy metal sources in the coastal soils developed from alluvial deposits using multivariate statistical methods. J. Hazard Mater. 164, 976–981.
Liang, J., Feng, C.T., Zeng, G.M., Gao, X., Zhong, M.Z., Li, X.D., Li, X., He, X.Y., Fang, Y.L., 2017. Spatial distribution and source identification of heavy metals in surface soils in a typical coal mine city, Lianyuan, China. Environ. Pollut. 225, 681–690.
Lindberg, S., Bullock, R., Ebinghaus, R., Engstrom, D., Feng, X.B., Fitzgerald, W., Pirrone, N., Prestbo, E., Seigneur, C., 2007. A synthesis of progress and uncertainties in attributing the sources of mercury in deposition. Ambio 36, 19–32.
Liu, Y., Lv, J.S., Zhang, B., Bi, J., 2013. Spatial multi-scale variability of soil nutrients in relation to environmental factors in a typical agricultural region, Eastern China. Sci. Total Environ. 450, 108–119.
Liu, Z., Jiang, L., Zhang, W., Zheng, F., Wang, M., Lin, H., 2008. Evolution of fertilization rate and variation of soil nutrient contents in greenhouse vegetable cultivation in Shandong. Acta Pedol. Sin. 45, 206–303.
Lu, A.X., Wang, J.H., Qin, X.Y., Wang, K.Y., Han, P., Zhang, S.Z., 2012. Multivariate and geostatistical analyses of the spatial distribution and origin of heavy metals in the agricultural soils in Shunyi, Beijing, China. Sci. Total Environ. 425, 66–74.
Lu, J.H., Jiang, P.P., Wu, L.S., Chang, A.C., 2008. Assessing soil quality data by positive matrix factorization. Geoderma 145, 259–266.
Lu, R.K., 2000. Analysis Method of Soil and Agricultural Chemistry. China Agricultural Science & Technology Press, Beijing.
Lu, R.K., Shi, Z.Y., Xiong, L.M., 1992. Cadmium contents of rock phosphates and phosphate fertilizers of China and their effects on ecological environment. Acta Pedol. Sin. 29, 150–157.
Luo, X.S., Xue, Y., Wang, Y.L., Cang, L., Xu, B., Ding, J., 2015. Source identification and apportionment of heavy metals in urban soil profiles. Chemosphere 127, 152–157.
Lv, J., Liu, Y., Zhang, Z., Dai, B., 2014. Multivariate geostatistical analyses of heavy metals in soils: spatial multi-scale variations in Wulian, Eastern China. Ecotoxicol. Environ. Saf. 107, 140–147.
Lv, J., Liu, Y., Zhang, Z., Dai, J., 2013. Factorial kriging and stepwise regression approach to identify environmental factors influencing spatial multi-scale variability of heavy metals in soils. J. Hazard Mater. 261, 387–397.
Lv, J., Yu, Y., 2018. Source identification and spatial distribution of metals in soils in a typical area of the lower Yellow River, eastern China. Environ. Sci. Pollut. Res. 25, 21106–21117.
Lv, J.S., Liu, Y., Zhang, Z.L., Dai, J.R., Dai, B., Zhu, Y.C., 2015a. Identifying the origins and spatial distributions of heavy metals in soils of Ju country (Eastern China) using multivariate and geostatistical approach. J. Soils Sediments 15, 163–178.
Lv, J.S., Liu, Y., Zhang, Z.L., Zhou, R.J., Zhu, Y.C., 2015b. Distinguishing anthropogenic and natural sources of trace elements in soils undergoing recent 10-year rapid urbanization: a case of Donggang, Eastern China. Environ. Sci. Pollut. Res. 22, 10539–10550.
Matheron, G., 1963. Principles of geostatistics. Econ. Geol. 58, 1246–1266.
Mortvedt, J.J., 1996. Heavy metal contaminants in inorganic and organic fertilizers. Fert. Res. 43, 55–61.
Nanos, N., Rodríguez Martin, J.A., 2012. Multiscale analysis of heavy metal contents in soils: spatial variability in the Duero river basin (Spain). Geoderma 189,

554–562.
Nziguheba, G., Smolders, E., 2008. Inputs of trace elements in agricultural soils via phosphate fertilizers in European countries. Sci. Total Environ. 390, 53–57.
Paatero, P., 1999. The multilinear engine - a table-driven, least squares program for solving multilinear problems, including the n-way parallel factor analysis model. J. Comput. Graph Stat. 8, 854–888.
Paatero, P., Hopke, P.K., 2009. Rotational tools for factor Analytic models. J. Chemom. 23, 91–100.
Paatero, P., Hopke, P.K., Song, X.H., Ramadan, Z., 2002. Understanding and controlling rotations in factor analytic models. Chemometr. Intell. Lab. Syst. 60, 253–264.
Paatero, P., Tapper, U., 1994. Positive matrix factorization - a nonnegative factor model with optimal utilization of error-estimates of data values. Environmetrics 5, 111–126.
Papritz, A., Schwierz, C., 2018. R Package Georob: Robust Geostatistical Analysis of Spatial Data. https://cran.r-project.org/web/packages/georob/index.html.
PriyaDarshini, S., Sharma, M., Singh, D., 2016. Synergy of receptor and dispersion modelling: quantification of PM10 emissions from road and soil dust not included in the inventory. Atmos. Pollut. Res. 7, 403–411.
Qu, M.K., Li, W.D., Zhang, C.R., Wang, S.Q., Yang, Y., He, L.Y., 2013. Source apportionment of heavy metals in soils using multivariate statistics and geostatistics. Pedosphere 23, 437–444.
Rodríguez Martín, J.A., Arias, M.L., Corbi, J.M.G., 2006. Heavy metals contents in agricultural topsoils in the Ebro basin (Spain). Application of the multivariate geoestatistical methods to study spatial variations. Environ. Pollut. 144, 1001–1012.
Rodríguez Martín, J.A., Ramos-Miras, J.J., Boluda, R., Gil, C., 2013. Spatial relations of heavy metals in arable and greenhouse soils of a Mediterranean environment region (Spain). Geoderma 200, 180–188.
Rodríguez Martin, J.A., De Arana, C., Ramos-Miras, J.J., Gil, C., Boluda, R., 2015. Impact of 70 years urban growth associated with heavy metal pollution. Environ. Pollut. 196, 156–163.
Rodríguez Martin, J.A., Nanos, N., 2016. Soil as an archive of coal-fired power plant mercury deposition. J. Hazard Mater. 308, 131–138.
Rodriguez, J.A., Nanos, N., Grau, J.M., Gil, L., Lopez-Arias, M., 2008. Multiscale analysis of heavy metal contents in Spanish agricultural topsoils. Chemosphere 70, 1085–1096.
Sajn, R., Halamic, J., Peh, Z., Galovic, L., Alijagic, J., 2011. Assessment of the natural and anthropogenic sources of chemical elements in alluvial soils from the Drava River using multivariate statistical methods. J. Geochem. Explor. 110, 278–289.
Siegel, F.R., 2001. Environmental Geochemistry of Potentially Toxic Metals. Springer, Berlin.
Sofowote, U.M., Allan, L.M., McCarry, B.E., 2010. A comparative study of two factor analytic models applied to PAH data from inhalable air particulate collected in an urban-industrial environment. J. Environ. Monit. 12, 425–433.
Sofowote, U.M., McCarry, B.E., Marvin, C.H., 2008. Source apportionment of PAH in Hamilton Harbour suspended sediments: comparison of two factor analysis methods. Environ. Sci. Technol. 42, 6007–6014.
Srivastava, R.K., Hutson, N., Martin, B., Princiotta, F., Staudt, J., 2006. Control of mercury emissions from coal-fired in electric utility boilers. Environ. Sci. Technol. 40, 1385–1393.
State Environmental Protection Administration of China, 1997. Environmental Quality Standard for Soils (GB15618-1995). Standards Press of China, Beijing.
Stout, S.A., Graan, T.P., 2010. Quantitative source apportionment of PAHs in sediments of little menomonee river, Wisconsin: weathered creosote versus urban background. Environ. Sci. Technol. 44, 2932–2939.
Thurston, G.D., Spengler, J.D., 1985. A quantitative assessment of source contributions to inhalable particulate matter pollution in metropolitan Boston. Atmos. Environ. 19, 9–25.
U.S. Environmental Protection Agency, 2014. EPA Positive Matrix Factorization (PMF) 5.0 Fundamentals and User Guide. https://www.epa.gov/sites/production/files/2015-02/documents/pmf_5.0_user_guide.pdf.
Vaccaro, S., Sobiecka, E., Contini, S., Locoro, G., Free, G., Gawlik, B.M., 2007. The application of positive matrix factorization in the analysis, characterisation and detection of contaminated soils. Chemosphere 69, 1055–1063.
Vanek, A., Grosslova, Z., Mihaljevic, M., Ettler, V., Trubac, J., Chrastny, V., Penizek, V., Teper, L., Cabala, J., Voegelin, A., Zadorova, T., Oborna, V., Drabek, O., Holubik, O., Houska, J., Pavlu, L., Ash, C., 2018. Thallium isotopes in metallurgical wastes/contaminated soils: a novel tool to trace metal source and behavior. J. Hazard Mater. 343, 78–85.
Vejahati, F., Xu, Z., Gupta, R., 2010. Trace elements in coal: associations with coal and minerals and their behavior during coal utilization – a review. Fuel 89, 904–911.
Wang, Q., Ma, Z., 2004. Heavy metals in chemical fertilizer and environmental risk. Rural Eco-Environ. 20, 62–64.
Wang, S.X., Zhang, L., Zhao, B., Meng, Y., Hao, J.M., 2012. Mitigation potential of mercury emissions from coal-fired power plants in China. Energy Fuel. 26, 4635–4642.
Webster, R., Oliver, M.A., 2007. Geostatistics for Environmental Scientists. Wiley, Chichester.
Wilhelm, S.M., 2001. Estimate of mercury emissions to the atmosphere from petroleum. Environ. Sci. Technol. 35, 4704–4710.
Wu, Q.R., Wang, S.X., Li, G.L., Liang, S., Lin, C.J., Wang, Y.F., Cai, S.Y., Liu, K.Y., Hao, J.M., 2016. Temporal trend and spatial distribution of speciated atmospheric mercury emissions in China during 1978-2014. Environ. Sci. Technol. 50, 13428–13435.
Xu, M.H., Yan, R., Zheng, C.G., Qiao, Y., Han, J., Sheng, C.D., 2004. Status of trace element emission in a coal combustion process: a review. Fuel Process. Technol. 85, 215–237.
Xue, J.L., Zhi, Y.Y., Yang, L.P., Shi, J.C., Zeng, L.Z., Wu, L.S., 2014. Positive matrix factorization as source apportionment of soil lead and cadmium around a battery plant (Changxing County, China). Environ. Sci. Pollut. Res. 21, 7698–7707.
Yang, Y.F., Huang, Q.F., Wang, Q., 2012. Ignoring emissions of Hg from coal ash and desulfurized Gypsum will lead to ineffective mercury control in coal-fired power plants in China. Environ. Sci. Technol. 46, 3058–3059.
Ying, H., Deng, M.H., Li, T.Q., Jan, J.P.G., Chen, Q.Q., Yang, X.E., He, Z.L., 2017. Anthropogenic mercury emissions from 1980 to 2012 in China. Environ. Pollut. 226, 230–239.
Zhang, L., Wang, S.X., Meng, Y., Hao, J.M., 2012a. Influence of mercury and chlorine content of coal on mercury emissions from coal-fired power plants in China. Environ. Sci. Technol. 46, 6385–6392.
Zhang, Y., Guo, C.S., Xu, J., Tian, Y.Z., Shi, G.L., Feng, Y.C., 2012b. Potential source contributions and risk assessment of PAHs in sediments from Taihu Lake, China: comparison of three receptor models. Water Res. 46, 3065–3073.
Zhao, S.L., Duan, Y.F., Wang, C.P., Liu, M., Lu, J.H., Tan, H.Z., Wang, X.B., Wu, L.T., 2017. Migration behavior of trace elements at a coal-fired power plant with different Boiler loads. Energy Fuel. 31, 747–754.
Zheng, J.Y., Ou, J.M., Mo, Z.W., Yin, S.S., 2011. Mercury emission inventory and its spatial characteristics in the Pearl River Delta region, China. Sci. Total Environ. 412, 214–222.
Zhong, X.L., Zhou, S.L., Zhu, Q., Zhao, Q.G., 2011. Fraction distribution and bioavailability of soil heavy metals in the Yangtze river Delta-A case study of Kunshan city in Jiangsu province, China. J. Hazard Mater. 198, 13–21.
Zhu, C.Y., Tian, H.Z., Cheng, K., Liu, K.Y., Wang, K., Hua, S.B., Gao, J.J., Zhou, J.R., 2016. Potentials of whole process control of heavy metals emissions from coal-fired power plants in China. J. Clean. Prod. 114, 343–351.